

Fabrication of CuInS₂ and Cu(In,Ga)S₂ thin films by a facile spray pyrolysis and their photovoltaic and photoelectrochemical properties

by Gunawan Gunawan

Submission date: 16-Nov-2020 12:09PM (UTC+0700)

Submission ID: 1447412989

File name: C-1_oke.pdf (1.38M)

Word count: 4355

Character count: 21263

Fabrication of CuInS_2 and Cu(In,Ga)S_2 thin films by a facile spray pyrolysis and their photovoltaic and photoelectrochemical properties

Cite this: DOI: 10.1039/c3cy00020f

Shigeru Ikeda,* Midori Nonogaki, Wilman Septina, Gunawan Gunawan, Takashi Harada and Michio Matsumura

Polycrystalline CuInS_2 chalcopyrite thin films were formed on a Mo-coated glass substrate by annealing of spray deposited precursor films in a sulfur atmosphere. Structural and photoelectrochemical analyses of CuInS_2 films obtained by annealing at 500 °C and 600 °C revealed that a well-defined crystalline film was obtained by the 600 °C annealing. Owing to these favorable properties, the solar cell with an $\text{Al:ZnO/CdS/CIS/Mo/glass}$ structure based on the 600 °C annealed CuInS_2 film showed higher conversion efficiency than that obtained on the cell derived from the 500 °C annealed CuInS_2 . Partial incorporation of Ga in the CuInS_2 film with a Ga/In ratio of ca. 0.2 to form a Cu(In,Ga)S_2 mixed crystal without any reduction of photoelectrochemical properties can be achieved by introduction of a Ga source in the sprayed solution. As a result, the solar cell based on the 600 °C annealed Cu(In,Ga)S_2 film showed the best conversion efficiency (5.8%) of the present sprayed chalcopyrite films. By introduction of a CdS thin layer followed by loading Pt deposits, moreover, the 600 °C annealed Cu(In,Ga)S_2 film worked as a photocathode for photoelectrochemical water splitting with applied bias potential of >0.65 V.

Received 7th January 2013,
Accepted 9th February 2013

DOI: 10.1039/c3cy00020f

www.rsc.org/catalysis

Introduction

Copper-based chalcogenide semiconductors have been the focus of intense investigation as photoabsorber layers in thin film solar cells. Among them, CuInS_2 (CIS) is one of the most important materials due to its high absorption coefficient of more than 10^4 cm^{-1} and optimum band gap energy (E_g) of 1.5 eV, 1,2 unlight absorption. Although the current record energy conversion efficiency of the CIS-based solar cell (12.5%) 3 is lower than that of the analogous Se-based compound, Cu(In,Ga)Se_2 (20.3%), 4 the use of CIS is advantageous because it does not require the addition of highly toxic Se, leading to realizing simple deposition apparatus and techniques to obtain high-quality films. Moreover, the fact that the partial replacement of In in CIS with isovalent Ga has shown to improve conversion efficiency up to 13% 5 suggests latent abilities of CIS-based sulfide films for substituents of existing selenide-based thin film solar cells.

Recently, many researchers have reported the possible applicability of Cu-based chalcogenides as p-type photocathodes

for photoelectrochemical (PEC) water splitting because of their appropriate band levels for water reduction and long-term stabilities confirmed in a solar cell application. In the PEC water splitting, it has been proved that introduction of n-type compounds to form p-n junction further improved their properties. Yokoyama *et al.* demonstrated appreciable improvements of PEC properties of Cu(In,Ga)Se_2 and $\text{Cu}_2\text{ZnSnS}_4$ photocathodes by formation of a heterojunction using n-type CdS and TiO_2 . 6,7 For the CIS-based PEC water splitting, we have also obtained a significant increase in the PEC response by introduction of p-n junction using CdS and ZnS thin layers. 8

Most of the efficient CIS-based solar cells were prepared by sputtering of Cu or In metallic precursor films followed by sulfurization with either H_2S or elemental sulfur. 3,5,9 This two-stage process is rather simple when compared to the fabrication of Cu(In,Ga)Se_2 , which requires a sophisticated high-vacuum evaporation technique. $^{4,10-15}$ However, it should be fairly advantageous that reliable and efficient solar cells based on the CIS absorber are prepared by non-vacuum processes instead of the expensive vacuum technique. Among a variety of non-vacuum processes, spray pyrolysis is an attractive method because of its easiness to deposit the CIS film in a large area. $^{16-19}$ Besides, composition of the films could be controlled effectively

Research Center for Solar Energy Chemistry, Osaka University,
1-3 Machikaneyama, Toyonaka 560-8531, Japan. E-mail: sikedai@chem.es.osaka-u.ac.jp;
Fax: 81 6 6850 6699; Tel: 81 6 6850 6699

by varying the concentration of the constituents in the spray solution: as a result, films with a wide range of composition can be prepared, unlike in any other deposition processes. These characteristic features motivated us to develop a fabrication process of the CIS thin film by the spray pyrolysis method. In this study, we attempted to fabricate efficient CIS-based solar cells and PEC water splitting systems. Specifically, effects of Ga incorporation on structural properties related to photovoltaic and PEC performances are discussed.

Experimental

An 1.5 cm^3 aqueous solution containing $0.09 \text{ mmol dm}^{-3}$ $\text{Cu}(\text{NO}_3)_2$, 0.1 mmol dm^{-3} $\text{In}(\text{NO}_3)_3$, and 0.8 mmol dm^{-3} thiourea ($\text{SC}(\text{NH}_2)_2$) was sprayed using an N_2 carrier. Deposition of CIS films was performed on a Mo-coated glass (Mo/glass) substrate heated at 300°C by using an AS ONE SLK1 hot plate. Prior to deposition, the Mo/glass substrate was precleaned by sonication in acetone and ultrapure water. The spray rate was fixed at $0.75 \text{ cm}^3 \text{ min}^{-1}$ by using a FUSO SEIKI Lumina STS-10SK atomizer. Thus-obtained CIS film composed from aggregates of fine particles (CIS_{ad}) was placed with 5.0 mg elemental sulfur in an evacuated Pyrex ampoule (*ca.* 160 cm^3) and annealed at 500 or 600°C for 10 min to facilitate crystallization; the thus-formed polycrystalline CIS films were labeled CIS₅₀₀ and CIS₆₀₀, respectively. For fabrication of the Ga-containing CIS film (Ga:CIS), a precursor solution containing $0.09 \text{ mmol dm}^{-3}$ $\text{Cu}(\text{NO}_3)_2$, $0.08 \text{ mmol dm}^{-3}$ $\text{In}(\text{NO}_3)_3$, $0.02 \text{ mmol dm}^{-3}$ $\text{Ga}(\text{NO}_3)_3$, and 10 mmol dm^{-3} thiourea ($\text{SC}(\text{NH}_2)_2$) was used, *i.e.*, 20% of $\text{In}(\text{NO}_3)_3$ was replaced with $\text{Ga}(\text{NO}_3)_3$. The sprayed Ga:CIS film (Ga:CIS_{ad}) was then annealed in the above sulfur containing Pyrex ampoule at 600°C for 10 min (labeled Ga:CIS₆₀₀).

Crystal structures of the films were analyzed by X-ray diffraction (XRD) using a Rigaku MiniF₂ X-ray diffractometer ($\text{CuK}\alpha$, Ni filter). Morphologies of the films was studied with scanning electron microscopy (SEM), using a Hitachi S-5000 FEG field emission scanning electron microscope at a voltage of 20 kV . Atomic compositions were analyzed by energy-dispersive X-ray (EDX) analysis using a Hitachi S-2250N EDX analyzer.

PEC properties of CIS and Ga:CIS films were measured in an aqueous solution containing 0.1 mol dm^{-3} $\text{Eu}(\text{NO}_3)_3$ as an electron scavenging electrolyte at $\text{pH } 4$.^{8,20} A Pyrex electrolytic cell having a flat window was used. Photocurrent responses of these films were measured under potentiostatic control using a three-electrode system with a Pt wire counter electrode and an Ag/AgCl reference electrode. Transient photocurrents were obtained by chopped illumination from a 300 W xenon lamp. Photocurrent onset potentials of CIS and Ga:CIS films were also determined by measuring transient photocurrents using the lock-in technique under 600 nm of monochromatic light illumination. All the photoelectrochemical measurements were performed under N_2 purging.

For the evaluation of solar cell properties, CIS and Ga:CIS films were processed to complete with an Al:ZnO/CdS/CIS(or Ga:CIS)/Mo/glass structure. The CdS buffer layer was deposited

by a chemical bath deposition (CBD).²¹ Then a transparent conductive oxide (TCO) layer of Al-doped ZnO (Al:ZnO) was deposited on the CdS surface by radio-frequency (RF)-magnetron sputtering. Current density–voltage (J – V) characteristics under simulated AM1.5 irradiation (100 mW cm^{-2}) were measured with a Bunkoh-Keiki CEP-015 photovoltaic measurement system.

For the PEC water splitting, CIS and Ga:CIS films were also modified with the CdS buffer layer by using the CBD method. Then platinum was photoelectrochemically deposited on the surface of these CdS-modified films in order to promote the hydrogen generation reaction. These modified films and RuO_2 counter electrode were placed within 1 cm of each other (no reference electrode) in 0.1 mol dm^{-3} aqueous Na_2SO_4 solution with pH adjusted to 13 using NaOH . Photoirradiation was performed using a 300 W xenon lamp.

Results and discussion

Fig. 1 shows XRD patterns of CIS_{ad}, CIS₅₀₀, CIS₆₀₀ and Ga:CIS₆₀₀ films. While the XRD pattern of the CIS_{ad} film showed almost no reflection except for a reflection of the Mo substrate (Fig. 1a), CIS₅₀₀ and CIS₆₀₀ films showed typical diffraction peaks assignable to the chalcopyrite CIS crystal, as shown in Fig. 1b and c.^{22,23} Relatively intense and sharp peaks observed on CIS₆₀₀ compared to those of CIS₅₀₀ indicates a high degree of crystalline nature of the CIS₆₀₀ film. The Ga:CIS₆₀₀ film also showed the same diffraction pattern assigned to the chalcopyrite structure, whereas each peak was slightly shifted to higher 2θ degrees than that of CIS₅₀₀ and CIS₆₀₀ films (Fig. 1d). From the fact that there are no other

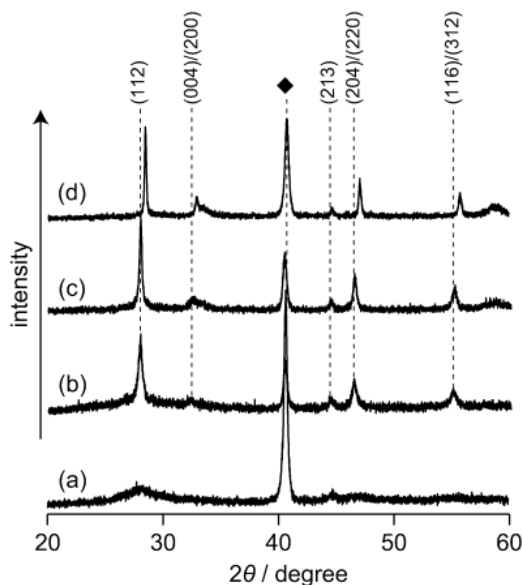


Fig. 1 X-ray diffraction patterns of (a) CIS_{ad}, (b) CIS₅₀₀, (c) CIS₆₀₀, and (d) Ga:CIS₆₀₀ films grown on a Mo/glass substrate. Diamond denotes diffraction peaks derived from the bottom Mo substrate.

crystalline phases included in any of the sample, the observed shifts of the XRD patterns are clear indications of the partial replacement of In with isovalent Ga to form a mixed crystal.

Fig. 2 shows cross-sectional SEM images of CIS_ad and annealed CIS and Ga:CIS films. The CIS_ad film showed a flat layer composed from aggregates of fine particles homogeneously laid up on the surface of the Mo substrate (Fig. 2a). The annealing induced crystalline growth to form micron-sized grains. It is clear that the angular-shaped CIS grain became larger upon increases in the annealing temperature, as shown in Fig. 2b and c. The Ga:CIS_600 film also indicated the formation of large micro-crystallites equivalent to the CIS_600 film, implying almost the similar topologies between these 600 °C annealed films irrespective of their compositional differences. In addition, bottom Mo layers of annealed samples formed a horizontal boundary line: the upper part of this line showed disappearance of typical columnar structure of Mo layer, implying the formation of a MoS₂ layer during sulfur-annealing.

As determined from EDX analyses, the atomic composition of CIS_ad was almost stoichiometric (*i.e.*, Cu/In/S = 1/1/2), while the composition ratio of the used precursor solution was in a slightly Cu-poor and a largely sulfur-rich from the ideal composition (*i.e.*, Cu/In/S = 0.9/1/8). The difference in the Cu/In ratio between the precursor solution and the CIS_ad film might be due to partial evaporation or blowoff of the In component during the spray deposition as discussed in the literature.²⁴ Similarly, the depletion of evaporation loss during the spray deposition should be considered for the sulfur source of thiourea used in this study. Moreover, thiourea has a function of a reduction reagent of divalent Cu ion into monovalent Cu to be included in the CIS film, resulting in the requirement of largely excess amounts of sulfur elements in the precursor solution. It is noted that there is no significant alteration of the Cu/In/S ratio observed in annealed CIS_500 and CIS_600 films, indicating homogeneous distribution of these three elements in CIS_ad. The requirement of the sulfur vapor during the 500 °C or 600 °C annealing is likely to be the suppression of sulfur evaporation from the film. The Ga:CIS film also provided similar tendencies, *i.e.*, the Cu/(In + Ga)/S (I/III/VI) ratio was almost stoichiometric regardless of the Cu poor/sulfur-rich composition of the precursor solution and almost the same composition was confirmed on the Ga:CIS_600 film. In addition, Ga content corresponding to In content in Ga:CIS_ad and Ga:CIS-600 films did not change from the precursor solution (Ga/In = 0.2), implying similar evaporation/blowoff behaviors between these elements during the spray deposition.

Fig. 3 shows typical linear sweep voltammetry (LSV) plots of CIS and Ga:CIS films measured in an aqueous Eu(NO₃)₃ solution under chopped illumination from a 300 W xenon lamp. While the CIS_ad film showed little photoresponse, all the annealed films gave appreciable cathodic photocurrents, indicating the p-type semiconductive features of these films. Among these annealed CIS films, CIS_600 showed slightly larger photocurrent than that of the CIS_500 film. The Ga:CIS_600 film induced comparable photocurrent response with that of the CIS_600 film in the present reaction condition.

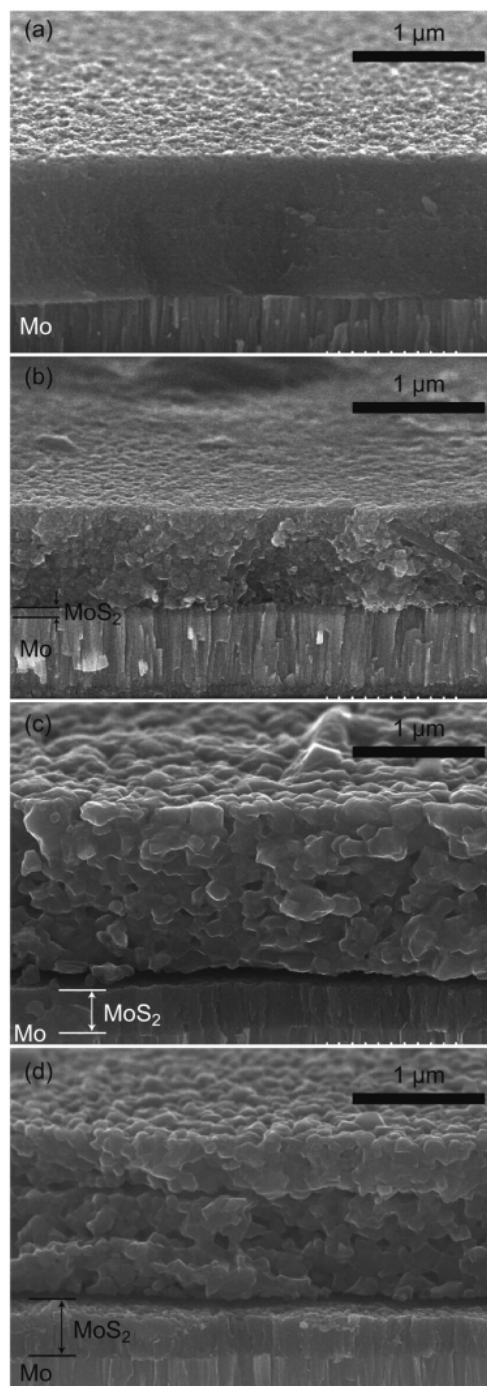


Fig. 2 Cross-sectional SEM images of (a) CIS_ad, (b) CIS_500, (c) CIS_600, and (d) Ga:CIS_600 films.

As shown in Fig. 4, corresponding photocurrent-potential curves of the CIS_600 and Ga:CIS_600 films measured under monochromatic light illumination (600 nm) using the lock-in

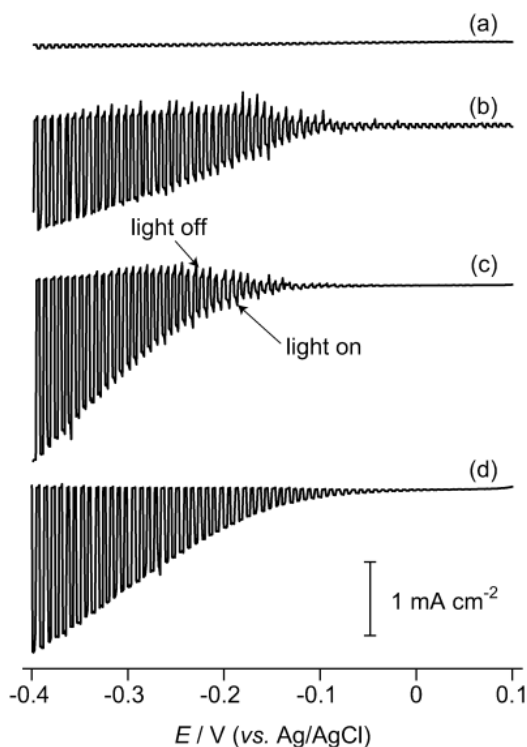


Fig. 3 LSV plots of (a) CIS_ad, (b) CIS_500, (c) CIS_600, and (d) Ga:CIS_600 films in 0.1 mol dm^{-3} europium nitrate under chopped illumination from a xenon lamp.

technique indicate similar photocurrent onset of *ca.* -0.05 V (*vs.* Ag/AgCl). Assuming that both of the films have similar doping densities and that onsets of the present p-type semiconductors occurred at potentials of *ca.* 0.2 V more negative than flat band potentials (E_{FB}),^{8,25} E_{FB} s of both CIS_600 and Ga:CIS_600 lie at *ca.* 0.15 V (*vs.* Ag/AgCl).

Fig. 5 shows J - V curves of CIS- and Ga:CIS-based solar cells with a device structure of Al:ZnO/CdS/CIS(or Ga:CIS)/Mo/glass. Cell parameters obtained from these J - V curves are summarized in Table 1. As expected from the above PEC experiment, the cell made from the CIS_ad film exhibited almost no diode characteristics, whereas solar cells based on annealed CIS and Ga:CIS films exhibited solar cell performances. A clear dependence of annealing temperature of the CIS film on solar cell was observed: the cell based on the CIS_600 film showed larger open circuit voltage (V_{OC}) and short circuit current (J_{SC}) than those of the cell based on the CIS_500 film. This resulted in achieving higher conversion efficiency (η) of the former solar cell (5.1%) than that of the latter solar cell (3.5%). Besides, the use of Ga:CIS_600 as the alternative photoabsorber induced appreciable increases in V_{OC} while it led to lowering the J_{SC} due mainly to the enlargement of E_{g} by the partial Ga incorporation (see below). It is noted that the Ga:CIS_600-based cell showed 5.8% of η , which is one of the best values for the sprayed chalcopyrite solar cells with a standard substrate configuration, though the CIS and Ga:CIS

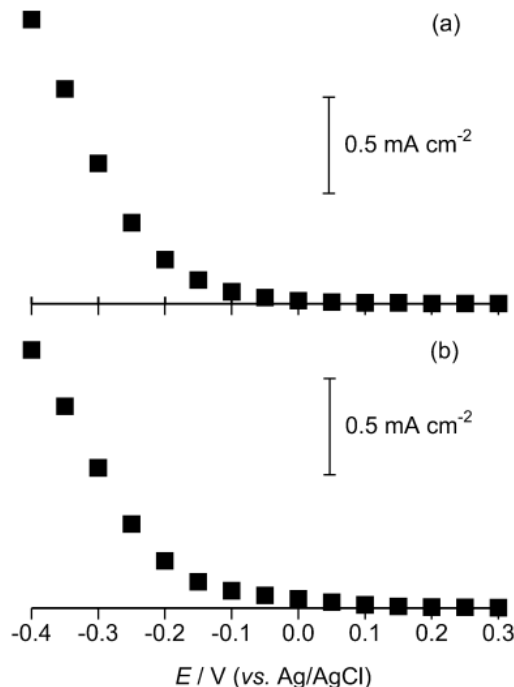


Fig. 4 Photocurrent-potential curves of (a) CIS_600 and (b) Ga:CIS_600 films in 0.1 mol dm^{-3} europium nitrate measured under monochromatic light illumination (600 nm) using the lock-in technique.

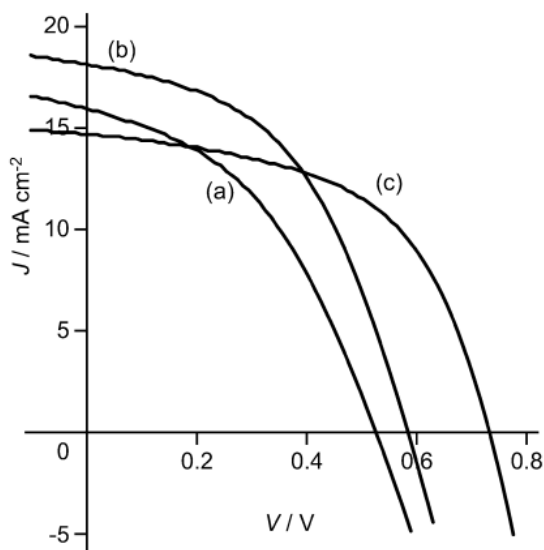


Fig. 5 J - V characteristics of Al:ZnO/CdS/CIS(or Ga:CIS)/Mo/glass cells. These cells were made from (a) CIS_500, (b) CIS_600, and (c) Ga:CIS_600 films.

solar cells prepared by other techniques have shown much higher η values.^{3,5} The appreciable improvement of fill factor (FF) from 0.44–0.48 (for annealed CIS-based cells) to 0.54 (for the

Table 1 Solar cell parameters obtained from illuminated *J*-*V* curves shown in Fig. 5

Photoabsorber	J_{SC}^a / mA cm ⁻²	V_{OC}^b / V	FF ^c (%)	η^d (%)
CIS_500	15.8	0.52	0.48	3.5
CIS_600	18.1	0.59	0.48	5.1
Ga:CIS_600	14.6	0.73	0.54	5.8

^a Short-circuit current density. ^b Open circuit voltage. ^c Fill factor. ^d Conversion efficiency.

Ga:CIS_600-based cell) should be the main cause such as a high η value on the cell, even though it composed of a relatively wide-gap photoabsorber.

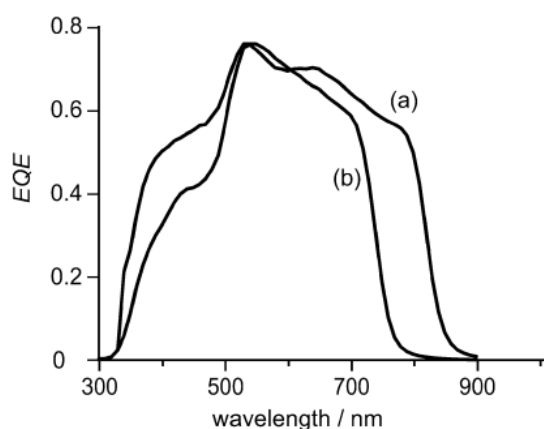
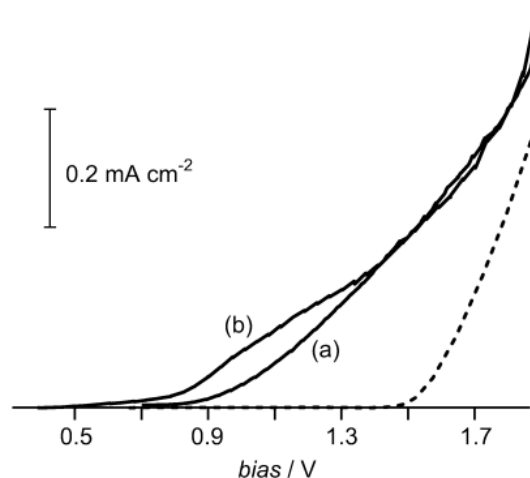
Fig. 6 shows external quantum efficiency (EQE) spectra of the CIS_600- and Ga:CIS_600-based cells in wavelength ranging from 300 nm to 1000 nm. Both of the EQE spectra increase gradually from the onset at *ca.* 350 nm to *ca.* 450 nm, steeply rising to *ca.* 520 nm, and then declining gradually to certain wavelengths (*ca.* 770 nm for the CIS_600-based cell and *ca.* 700 nm for the Ga:CIS_600-based cell). The reduction of EQE response in the short wavelength region is due to absorption losses in the window (Al:ZnO) and buffer (CdS) layers. On the other hand, the gradual weakening of EQE responses in relatively long wavelength regions indicates a loss of deeply absorbed photons due to poor minority carrier diffusion length and/or insufficient penetration of depletion width into the absorber.^{26,27} Such a failure would be caused by a high majority carrier concentration of the photoabsorbers, *i.e.*, defect densities present in CIS_600 and Ga:CIS_600 films are in excess from an optimum amount.

The EQE spectrum of the Ga:CIS_600-based cell showed appreciable blue-shift of the onset wavelength due to the enlargement of E_g by the partial replacement of In with Ga: the CIS-based cell showed the EQE onset at 860 nm, which corresponded to the reported E_g value of CIS (1.48 eV),^{1,2} whereas the Ga:CIS_600-based cell gave the 780 nm onset corresponding to 1.68 of E_g . Since E_g of the pure Ga analogue

(*i.e.*, CuGaS₂) is known to be 2.43 eV,²⁸ the E_g value of Ga:CIS with 20% Ga content along with that of In can be estimated to be 1.69 eV when a linear increase of E_g with the Ga content in Ga:CIS from zero (CIS) to 100% (CuGaS₂) is assumed. The value also coincides well with the E_g value of the present Ga:CIS_600 film.

PEC water splitting was performed by using CdS-modified CIS_600 and Ga:CIS_600 films as photocathodes and a RuO₂ counter electrode (with no reference). It should be noted that platinum nanoparticles were photoelectrochemically deposited on these modified CIS_600 and Ga:CIS_600 films in order to induce efficient hydrogen production. Typical photocurrent-bias voltage curves thus-obtained are shown in Fig. 7a and b. For comparison, the current-bias voltage curve of water electrolysis using a Pt cathode and the RuO₂ counter electrode (anode) is also shown in this figure (dotted line). The onset bias voltage of the water electrolysis was *ca.* 1.5 V in the present electrochemical setup. Since the water reduction on the Pt cathode should occur without appreciable overpotential, the requirement of excess bias potential compared to the thermodynamic demand (1.23 V) is likely to be due to the overpotential of water oxidation on the RuO₂ anode. In comparison with the onset of water electrolysis, the onset bias voltage significantly reduced when the modified CIS_600 photocathode was used, *i.e.*, PEC water splitting induced by applying bias potentials of more than 0.80 V (Fig. 7a). Moreover, further reduction of the required bias potential (>0.65 V) achieved when the modified Ga:CIS_600 was employed as the photocathode, as shown in Fig. 7b.

The above solar cell and PEC water splitting properties suggest that there seems to be a reciprocal relationship between the V_{OC} values of the solar cell and the required bias voltages of the PEC water splitting. In order to construct a "non-bias" PEC water splitting system by the combination of photoanodes which evolve oxygen and photocathodes which evolve

**Fig. 6** External quantum efficiency (EQE) spectra of (a) CIS_600- and (b) Ga:CIS_600-based solar cells.**Fig. 7** Photocurrent-bias voltage curves of (a) CIS_600 and (b) Ga:CIS_600 films modified with CdS buffer layer and Pt deposits. Dotted line denotes the current-potential curve of water electrolysis using a Pt cathode.

hydrogen,²⁹ the reduction of bias voltage of each photoelectrode is important. Thus, the development of the Cu-chalcogenide-based solar cell with high V_{OC} is desirable for PEC water splitting. Further studies along this line are now in progress.

Conclusions

In this study, we have proved possible fabrication of CIS- and Ga:CIS-based solar cells by using a facile non-vacuum technique, spray pyrolysis. The conversion efficiencies on these cells achieved a high level among the chalcopyrite solar cells fabricated by spray methods. By using the p-n junction formation in solar cell technology, moreover, we can demonstrate PEC water splitting whilst applying relatively low bias potentials, specifically on the Ga:CIS-based photocathode. Since the present spray pyrolysis is advantageous for the survey of new materials, we can expect to find efficient p-n junctions for induction of PEC water splitting with relatively low overpotentials by using this technique.

Acknowledgements

This work was partially supported by New Energy and Industrial Technology Development Organization (NEDO).

Notes and references

- 1 M. Krunk, O. Bijakina, T. Varema, V. Mikli and E. Mellikov, *Thin Solid Films*, 1999, **338**, 125.
- 2 M. A. Green, K. Emery, D. L. King, S. Igari and W. Warta, *Progr. Photovolt.: Res. Appl.*, 2002, **10**, 355.
- 3 J. Klaery, J. Bruns, R. Henninger, K. Siemer, R. Klenk, K. Ellmer and D. Bräunig, *Semicond. Sci. Technol.*, 1998, **13**, 1456.
- 4 P. Jackson, D. Hariskos, E. Lotter, S. Paetel, R. Wuerz, R. Menner, W. Wischmann and M. Powalla, *Prog. Photovolt.*, 2011, **19**, 894.
- 5 S. Merdes, B. Johnson, R. Sáez-Araoz, A. Ennaoui, J. Klaer, I. Lauermann, R. Mainz, A. Meeder and R. Klenk, *MRS Online Proc. Libr.*, 2011, **1165**, 1165-M05-15.
- 6 D. Yokoyama, T. Minegishi, K. Maeda, M. Katayama, J. Kubota, A. Yamada, M. Konagai and K. Domen, *Electrochem. Commun.*, 2010, **12**, 851.
- 7 D. Yokoyama, T. Minegishi, K. Jimbo, T. Hisatomi, G. Ma, M. Katayama, J. Kubota, H. Katagiri and K. Domen, *Appl. Phys. Express*, 2010, **3**, 101202.
- 8 S. Ikeda, T. Nakamura, S. M. Lee, T. Yagi, T. Harada, T. Minegishi and M. Matsumura, *ChemSusChem*, 2011, **4**, 262.
- 9 R. Klenk, J. Klaer, R. Scheer, M. C. Lux-Steiner, I. Luck, N. Meyer and U. Rühle, *Thin Solid Films*, 2004, **480–481**, 509.
- 10 M. Contreras, B. Egaas, R. Ramanathan, J. Hiltner, A. Swartzlander, F. Hasoon and R. Noufi, *Progr. Photovolt.: Res. Appl.*, 1999, **7**, 311.
- 11 H.-W. Schock and R. Noufi, *Progr. Photovolt.: Res. Appl.*, 2000, **8**, 151.
- 12 M. Powalla and B. Dimmler, *Sol. Energy Mater. Sol. Cells*, 2003, **75**, 12.
- 13 F. Karg, *Sol. Energy Mater. Sol. Cells*, 2001, **66**, 645.
- 14 G. Palm, V. Probst and F. H. Karg, *Sol. Energy*, 2004, **77**, 757.
- 15 R. Sáez-Araoz, D. Abou-Ras, T. P. Niesen, A. Neisser, K. Wilhelmi, M. C. Lux-Steiner and A. Ennaoui, *Thin Solid Films*, 2009, **517**, 2300.
- 16 I. Oja, M. Nanu, A. Katerski, M. Krunk, A. Mere, J. Raudoja and A. Goossens, *Thin Solid Films*, 2005, **480–481**, 82.
- 17 M. Krunk, O. Kijatkina, A. Mere, T. Varema, I. Oja and V. Mikli, *Sol. Energy Mater. Sol. Cells*, 2005, **87**, 207.
- 18 A. Katerski, A. Mere, V. Kazlauskienė, J. Miskinis, A. Saar, L. Matisen, A. Kikas and M. Krunk, *Thin Solid Films*, 2008, **516**, 7110.
- 19 C. Camus, N. A. Allsop, S. E. Gledhill, W. Böhne, J. Röhrich, I. Lauermann, M. C. Lux-Steiner and C. H. Fischer, *Thin Solid Films*, 2008, **516**, 7026.
- 20 S. M. Lee, S. Ikeda, T. Yagi, T. Harada, A. Ennaoui and M. Matsumura, *Phys. Chem. Chem. Phys.*, 2011, **13**, 6662.
- 21 S. Ikeda, R. Kamai, T. Yagi and M. Matsumura, *J. Electrochem. Soc.*, 2010, **157**, B99.
- 22 T. Todorov, E. Cordoncillo, J. F. Sanchez-Royo, J. Carda and P. Escibano, *Chem. Mater.*, 2006, **18**, 3145.
- 23 E. Izquierdo-Roca, A. Pérez-Rodríguez, J. R. Morante, J. Álvarez-García, L. Calvo-Barrio, V. Bermudez, P. P. Grand, L. Parissi, C. Broussillon and O. Kerrec, *J. Appl. Phys.*, 2008, **103**, 123109.
- 24 M. Krunk, V. Mikli, O. Bijakina and E. Mellikov, *Appl. Surf. Sci.*, 1999, **142**, 356.
- 25 J. J. Scragg, P. J. Dale, L. M. Peter, G. Zoppi and I. Fobes, *Phys. Status Solidi B*, 2008, **245**, 1772.
- 26 I. Repins, C. Beall, N. Vora, C. DeHart, D. Kuciauskas, P. Dippo, B. To, J. Mann, W. C. Hsu, A. Goodrich and R. Noufi, *Sol. Energy Mater. Sol. Cells*, 2012, **101**, 154.
- 27 S. M. Lee, S. Ikeda, Y. Otsuka, T. Harada and M. Matsumura, *Electrochim. Acta*, 2012, **79**, 189.
- 28 R. Kaigawa, A. Ohya, T. Wada and R. Klenk, *Thin Solid Films*, 2007, **515**, 6260.
- 29 A. J. Nozik, *Appl. Phys. Lett.*, 1977, **30**, 567.

Fabrication of CuInS₂ and Cu(In,Ga)S₂ thin films by a facile spray pyrolysis and their photovoltaic and photoelectrochemical properties

ORIGINALITY REPORT

9%

SIMILARITY INDEX

7%

INTERNET SOURCES

7%

PUBLICATIONS

3%

STUDENT PAPERS

PRIMARY SOURCES

- | | | |
|--|--|--|
| <div style="background-color: red; color: white; width: 40px; height: 40px; display: flex; align-items: center; justify-content: center; margin: 0 auto;">1</div> | <p>Mejda Ajili, Michel Castagné, Najoua Kamoun Turki. "Spray solution flow rate effect on growth, optoelectronic characteristics and photoluminescence of SnO₂:F thin films for photovoltaic application", Optik, 2015</p> <p>Publication</p> | <div style="font-size: 2em;">1</div> % |
| <hr/> | | |
| <div style="background-color: purple; color: white; width: 40px; height: 40px; display: flex; align-items: center; justify-content: center; margin: 0 auto;">2</div> | <p>etds.lib.ncku.edu.tw</p> <p>Internet Source</p> | <div style="font-size: 2em;">1</div> % |
| <hr/> | | |
| <div style="background-color: purple; color: white; width: 40px; height: 40px; display: flex; align-items: center; justify-content: center; margin: 0 auto;">3</div> | <p>Sean P. Berglund, Heung Chan Lee, Paul D. Núñez, Allen J. Bard, C. Buddie Mullins. "Screening of transition and post-transition metals to incorporate into copper oxide and copper bismuth oxide for photoelectrochemical hydrogen evolution", Physical Chemistry Chemical Physics, 2013</p> <p>Publication</p> | <div style="font-size: 2em;">1</div> % |
| <hr/> | | |
| <div style="background-color: teal; color: white; width: 40px; height: 40px; display: flex; align-items: center; justify-content: center; margin: 0 auto;">4</div> | <p>nano.uantwerpen.be</p> <p>Internet Source</p> | <div style="font-size: 2em;">1</div> % |
-

5

Bär, Marcus, Joachim Klaer, Lothar Weinhardt, Regan G. Wilks, Stefan Krause, Monika Blum, Wanli Yang, Clemens Heske, and Hans-Werner Schock. "Cu_{2-x}S Surface Phases and Their Impact on the Electronic Structure of CuInS₂ Thin Films - A Hidden Parameter in Solar Cell Optimization", Advanced Energy Materials, 2013.

Publication

<1 %

6

Gautron, E., M. Buffière, S. Harel, L. Assmann, L. Arzel, L. Brohan, J. Kessler, and N. Barreau. "Microstructural characterization of chemical bath deposited and sputtered Zn(O,S) buffer layers", Thin Solid Films, 2013.

Publication

<1 %

7

Shufang Zhang, Xudong Yang, Kun Zhang, Han Chen, Masatoshi Yanagida, Liyuan Han. "Effects of 4-tert-butylpyridine on the quasi-Fermi levels of TiO₂ films in the presence of different cations in dye-sensitized solar cells", Physical Chemistry Chemical Physics, 2011

Publication

<1 %

8

Submitted to South Dakota Board of Regents

Student Paper

<1 %

9

B. J. Babu, B. Egaas, S. Velumani. "Selenization of CIS and CIGS layers deposited by chemical

<1 %

spray pyrolysis", Journal of Materials Science:
Materials in Electronics, 2018

Publication

10

www.science.gov

Internet Source

<1 %

11

eprints.soton.ac.uk

Internet Source

<1 %

12

Taunier, S.. "Cu(In,Ga)(S,Se)² solar cells and modules by electrodeposition", Thin Solid Films, 20050601

Publication

<1 %

13

www.intechopen.com

Internet Source

<1 %

14

J. B. CHU, H. B. ZHU, Z. A. WANG, Z. Q. BIAN, Z. SUN, Y. W. CHEN, S. M. HUANG. " DEPOSITION OF SINGLE-PHASE THIN FILMS UNDER LOW VACUUM LEVEL BY A TWO-STAGE GROWTH TECHNIQUE ", Surface Review and Letters, 2012

Publication

<1 %

15

Jianmin Li, Jiabin Niu, Xiao Wu, Yifan Kong, Jinlong Gao, Jiakuan Zhu, Qiang Li, Lan Huang, Shijin Wang, Zheng Chi, Xudong Xiao. " Effects of Laser - Scribed Mo Groove Shape on Highly Efficient Zn(O,S) - Based Cu(In,Ga)Se Solar Modules ", Solar RRL, 2020

Publication

<1 %

16 Klenk, R.. "Development of CuInS₂-based solar cells and modules", Solar Energy Materials and Solar Cells, 201106 Publication <1 %

17 media.proquest.com Internet Source <1 %

18 worldwidescience.org Internet Source <1 %

19 pnrresolution.org Internet Source <1 %

20 pubs.rsc.org Internet Source <1 %

21 www.hindawi.com Internet Source <1 %

22 A. - M. Gurban, B. Prieto - Simón, J. - L. Marty, T. Noguer. "Malate Biosensors for the Monitoring of Malolactic Fermentation: Different Approaches", Analytical Letters, 2006 Publication <1 %

23 Cheng, K.W.. "Effect of [Cu]/[Cu+In] ratio in the solution bath on the growth and physical properties of CuInS₂ film using one-step electrodeposition", Journal of Electroanalytical Chemistry, 20111001 Publication <1 %

24

www.european-mrs.com

Internet Source

<1 %

25

Dittrich, H.. "Sulfosalts - A new class of compound semiconductors for photovoltaic applications", Thin Solid Films, 20070531

Publication

<1 %

26

Wakita, K.. "Temperature dependence of time-resolved photoluminescence of bound excitons in CuInS₂ crystals", Thin Solid Films, 20050601

Publication

<1 %

Exclude quotes Off

Exclude matches Off

Exclude bibliography Off

Fabrication of CuInS₂ and Cu(In,Ga)S₂ thin films by a facile spray pyrolysis and their photovoltaic and photoelectrochemical properties

GRADEMARK REPORT

FINAL GRADE

/0

GENERAL COMMENTS

Instructor

PAGE 1

PAGE 2

PAGE 3

PAGE 4

PAGE 5

PAGE 6